Allosteric regulation by cytoplasmic Ca^{2+} and IP_3 of the gating of IP_3 receptors in permeabilized guinea-pig vascular smooth muscle cells

Kenzo Hirose, Shiro Kadowaki and Masamitsu Iino

Department of Pharmacology, Faculty of Medicine, The University of Tokyo and CREST, Japan Science and Technology Corporation, Tokyo 113, Japan

(Received 14 July 1997; accepted after revision 11 September 1997)

1. The potentiation by Ca^{2+} of inositol 1,4,5-trisphosphate (IP_3)-induced Ca^{2+} release was studied by measuring luminal Ca^{2+} concentrations of the Ca^{2+} stores using a fluorescent Ca^{2+} indicator, furaptra, in permeabilized smooth muscle cells.

2. Ca^{2+} release at 10 μM IP_3 was potentiated by an increase in the cytoplasmic Ca^{2+} concentration in the presence of 10 mM EGTA. This effect was not due to the pharmacological effect of EGTA, because changes in the EGTA concentration at a constant Ca^{2+} concentration had no effect on the Ca^{2+} release rate.

3. With an increase in the cytoplasmic Ca^{2+} concentration from 30 to 630 nM, the Ca^{2+} release rate at a saturating IP_3 concentration increased 110-fold and the EC_{50} for IP_3 increased from 0·07 to 1·0 μM. It was also indicated that the relationship between Ca^{2+} concentration and Ca^{2+} release rate was shifted towards higher Ca^{2+} concentrations at higher IP_3 concentrations.

4. These results suggest that IP_3 and submicromolar concentrations of Ca^{2+} allosterically lower the affinity of the IP_3 receptor for each other and are both required for IP_3 receptor activation. These properties enable the IP_3 receptors to detect simultaneous increases in IP_3 and Ca^{2+} concentrations.

Agonist-activated cells often show intermittent increases in intracellular Ca^{2+} concentration, or Ca^{2+} oscillations, which are usually accompanied by intracellular and/or intercellular Ca^{2+} waves. These properties of the Ca^{2+} signalling in stimulated cells resemble the membrane action potentials that exhibit temporal oscillations and propagate as spatial waves. In analogy to the generation of action potentials in excitable cells, it has been thought that the underlying mechanism of the Ca^{2+} waves and oscillations is the presence of a Ca^{2+}-based excitable medium, in which an increase in Ca^{2+} concentration activates release of Ca^{2+} from its stores in a regenerative manner. Although the mechanism of these complex Ca^{2+} mobilization patterns is not fully understood, Ca^{2+}-mediated feedback regulation of ryanodine receptor (RyR) or IP_3 receptor (IP_3R) activity is likely to be a key component of the excitable medium in many types of cells (Berridge, 1993). Indeed, RyR has been shown to function by Ca^{2+}-induced Ca^{2+} release (CICR) and this seems to be the mechanism of Ca^{2+} oscillations and waves in striated muscle cells (Endo, Tanaka & Ogawa, 1970; Takamatsu & Wier, 1990). It has been shown that IP_3R activity is also controlled by changes in the cytoplasmic Ca^{2+} concentration, in a biphasic manner: Ca^{2+} at submicromolar concentrations potentiates IP_3-induced Ca^{2+} release, while Ca^{2+} at higher concentrations inhibits it (Iino, 1990; Bezprozvanny, Watras & Ehrlich, 1991; Finch, Turner & Goldin, 1991; Bootman, Missiaen, Parys, De Smedt & Casteels, 1995). Furthermore, it has been demonstrated that IP_3 induces Ca^{2+} release from the Ca^{2+} stores in permeabilized smooth muscle cells in a regenerative manner, via the Ca^{2+}-mediated feedback regulation of IP_3R activity (Iino & Endo, 1992). However, the quantitative aspects of the IP_3R activation are not fully understood and it is not yet known how Ca^{2+} potentiates IP_3R activity.

To elucidate the mechanism of the Ca^{2+}-mediated potentiation of IP_3R activity, we analysed the Ca^{2+} dependence of IP_3-induced Ca^{2+} release using a recently developed method for real-time measurement of the luminal Ca^{2+} concentrations of the Ca^{2+} stores (Hirose & Iino, 1994). Our results show that Ca^{2+} potentiates IP_3R activity not by increasing IP_3R affinity for IP_3, but because it is absolutely required for IP_3R activity. This property enables the IP_3R to detect a simultaneous increase in the concentrations of two different intracellular signals: Ca^{2+} and IP_3.

METHODS

Preparation

Guinea-pigs (weight, ~300 g each) were stunned and exsanguinated. Segments of the portal vein were dissected from the liver and transferred to a dissecting chamber containing physiological salt solution (PSS). The vein was longitudinally cut open, and the endothelium was removed by rubbing with a small piece of paper. Thin smooth muscle bundles (3 mm in length, 150–250 μm in width and 50–60 μm in thickness) were obtained after removal of the adventitial tissue, and were tied to a thin stainless steel wire. We employed furaptra as an fluorescent indicator of Ca^{2+} concentration within the Ca^{2+} stores, because furaptra is a low-affinity Ca^{2+} indicator (~48 μM at ionic strength of 0·2 M, pH 7; K. Hirose & M. Iino, unpublished observation) and is thus suitable for measurement of the high Ca^{2+} concentrations expected inside the Ca^{2+} stores. The specimens were incubated in PSS containing 20–40 μM furaptra-AM (the acetoxymethyl ester form of furaptra) for 3–5 h at 35 °C. The furaptra-loaded fibre bundles were then permeabilized by incubation with 40 μM β-escin in relaxing solution to wash out the furaptra in the cytoplasm. This procedure enables measurement of the concentrations of Ca^{2+} within the intracellular organelles.

Experimental apparatus

The apparatus used for the experiments has been described previously (Hirose & Iino, 1994). Briefly, the specimen tied to the stainless steel wire was inserted into a small glass capillary (i.d. 400 μm) which was attached to the cuvette holder of a fluorescence spectrophotometer (CAF110, JASCO, Tokyo, Japan). The specimen was then illuminated with 340 nm and 375 nm wavelength light alternately and the emitted light was directed to a photomultiplier tube. The ratio of the fluorescence intensity at 340 nm excitation to that at 380 nm excitation was used as an indicator of the luminal Ca^{2+} concentration. One end of the glass capillary was connected to the common output of an electrically driven valve which had sixteen channel inputs.

The other end of the capillary was connected to two peristaltic pumps. One of the pumps was used to change the solution around the specimen rapidly (within 1 s). Continuous slow flow of the solution over the specimen was driven by another peristaltic pump.

Protocol

The solution within the capillary was sequentially exchanged to load and release Ca^{2+} from the Ca^{2+} stores of the specimen. After the fibre bundle was bathed in relaxing solution for 60 s, Ca^{2+} was loaded into the Ca^{2+} stores by application of loading solution, containing 100 nM Ca^{2+} and 0·5 mM MgATP, for 25 s. The Ca^{2+} loading was terminated by the exchange of loading solution with G10RMg0 solution, which contained 10 mM EGTA with neither Ca^{2+} nor MgATP. (All the solutions used in the subsequent steps also contained no MgATP.) The G10RMg0 solution was exchanged with G1RMg0 solution in which the concentration of EGTA was reduced to 1 mM. After 30 or 60 s, the concentration of Ca^{2+} was increased by application of assay solution containing 10 mM EGTA and various amounts of Ca^{2+}. IP_3 (30 nM–10 μM) was subsequently applied for 120 s in the same solution. The Ca^{2+} stores were then completely depleted by 120 s application of 10 μM IP_3 in the presence of 300 nM Ca^{2+}. After IP_3 and Ca^{2+} were washed out for 60 s, the specimen was again bathed in the relaxing solution to start a new run. The Ca^{2+} loading and Ca^{2+} release sequences were repeated several times for each specimen.

Measurement of IP_3R activity

The IP_3R activity was evaluated in terms of the initial Ca^{2+} release rate as described previously (Hirose & Iino, 1994). The observed changes in ratio of fluorescence intensities were normalized so that 1 and 0 corresponded, respectively, to the values just before the application of IP_3 and after complete depletion by 10 μM IP_3 for 120 s.

The initial part of the normalized time course, where the normalized fluorescence ratio signal remained between 1·0 and 0·8, was fitted by a single exponential function, e^{-rt}. The rate constant, r, thus estimated was used as an index of the extent of IP_3R activation.

Solutions

The solutions used for the present experiments were essentially the same as those previously described (Iino, 1990; Hirose & Iino, 1994). PSS contained (mM): 150 NaCl, 4 KCl, 1 $MgCl_2$, 2 $CaCl_2$, 5·6 glucose and 5 Hepes (pH 7·4). Relaxing solution contained (mM): 116 potassium methanesulphonate, 3·31 ATP, 0·554 magnesium methanesulphonate and 1 EGTA. Loading solution contained (mM): 112 potassium methanesulphonate, 3·32 ATP, 0·564 magnesium methanesulphonate, 1·96 CaEGTA and 8·04 EGTA. G10RMg0 solution contained 112 mM potassium methanesulphonate and 10 mM EGTA. CaG10RMg0 solution contained 112 mM potassium methanesulphonate and 10 mM CaEGTA. G1RMg0 contained 139 mM potassium methanesulphonate and 1 mM EGTA. All solutions except for PSS contained (mM): 20 NaN_3, 1 EGTA and 20 Pipes (pH 7·0). Assay solutions containing Ca^{2+} at various concentrations were prepared by mixing CaG10RMg0 solution and G10RMg0 solution at appropriate ratios. The ratios of the volume of CaG10RMg0 solution to the total volume of the assay solution were: 0·072, 0·196, 0·329, 0·434 and 0·608 for 30, 100, 200, 300 and 630 nM Ca^{2+}, respectively.

Chemicals

Furaptra-AM (mag-fura-2 AM) was purchased from Molecular Probes, and IP_3 from Dojin-do (Kumamoto, Japan). All other drugs were purchased either from Sigma or from Wako Chemicals (Tokyo, Japan).

RESULTS

Ca^{2+}-mediated potentiation of IP_3-induced Ca^{2+} release

Figure 1*A* shows the time courses of Ca^{2+} release from the Ca^{2+} stores of permeabilized smooth muscle cells, following application of 10 μM IP_3 at various cytoplasmic Ca^{2+} concentrations in the absence of MgATP. The Ca^{2+} release rate increased as the concentration of Ca^{2+} was increased, within the range used in the experiments (30–630 nM). Figure 1*B* shows the results compiled from five preparations. It can be seen that the Ca^{2+} release rate at 10 μM IP_3 increased markedly with increasing cytoplasmic Ca^{2+} concentration. This observation is consistent with previous reports based on different methods (Iino, 1990; Bezprozvanny *et al.* 1991; Finch *et al.* 1991). In the absence of IP_3, changes in cytoplasmic Ca^{2+} concentration had no effect on the time course of Ca^{2+} release (not shown). Thus, the observed potentiation of Ca^{2+} release by Ca^{2+} did not involve Ca^{2+}-induced Ca^{2+} release (CICR) via ryanodine receptors (RyRs). This result is consistent with the results of a previous study showing CICR occurs only when the cytoplasmic Ca^{2+} concentration exceeds 1 μM in smooth muscle cells (Iino, 1989).

We did not measure the Ca^{2+} release rate at higher cytoplasmic Ca^{2+} concentrations (> 1 μM), at which Ca^{2+} has been reported to inhibit IP_3-induced Ca^{2+} release (Iino, 1990). This is because application of high concentrations of Ca^{2+} (> 1 μM) alone increased the fluorescence intensity ratio of furaptra even in the absence of MgATP. The change in the fluorescence intensity ratio was not due to passive influx of Ca^{2+} into the Ca^{2+} stores, because the increase in the fluorescence intensity ratio was reversed upon removal of Ca^{2+} in the absence of IP_3. Therefore, the change in the furaptra fluorescence intensity ratio at high concentrations of Ca^{2+} (> 1 μM) is likely to be due to the binding of Ca^{2+} to compartmentalized furaptra which is accessed only at high cytoplasmic Ca^{2+} concentrations. Although this compartment might be mitochondria, which are known to respond to high concentrations of Ca^{2+} and have been shown to accumulate Ca^{2+}-sensitive fluorescent dyes including furaptra (Hoffer, Schlue, Curci & Machen, 1995; Golovina & Blaustein, 1997), we did not study the possibility further. We thus analysed the Ca^{2+} release only at < 1 μM Ca^{2+}, ensuring the observed time courses were free from such effects.

Effect of EGTA on Ca^{2+} release rate

Ca^{2+} chelating agents such as BAPTA have been reported to inhibit the binding of IP_3 to its receptor, resulting in attenuation of Ca^{2+} release even at a constant Ca^{2+} concentration (Richardson & Taylor, 1993). This pharmacological effect of Ca^{2+} chelating agents might interfere with the observed potentiation by changing the Ca^{2+} concentration, because the concentration of Ca^{2+}-unbound EGTA, which has been reported to inhibit IP_3 binding more strongly than Ca^{2+}-bound EGTA, decreased when the Ca^{2+} concentration was raised in the experiments presented in Fig. 1. Although the inhibitory effect of EGTA on IP_3 binding has been reported to be weaker than those of other chelators, we tested the possibility that the potentiation of Ca^{2+} release was due to the pharmacological effects of EGTA.

We found that the potentiating effect of Ca^{2+} (300 nM) did not change when the total EGTA concentration was increased from 10 mM to 14·3 mM or decreased to 4·3 mM so that the concentration of Ca^{2+}-unbound or Ca^{2+}-bound EGTA, respectively, was the same as that at 100 nM Ca^{2+} with a 10 mM total EGTA concentration (Fig. 2). The results show that the extent of potentiation depends only on the free Ca^{2+} concentration and is independent of the concentration of Ca^{2+}-bound and Ca^{2+}-unbound EGTA, and indicate that the observed potentiation by Ca^{2+} of IP_3-induced Ca^{2+} release is not the result of the inhibitory effect of EGTA on IP_3 binding.

Effect of Ca^{2+} on IP_3 sensitivity of Ca^{2+} release via IP_3R

We then attempted to elucidate the mechanism by which Ca^{2+} potentiates IP_3R activity. We first considered two extreme cases. One possible mechanism is that Ca^{2+} increases the affinity of IP_3R for IP_3. The other is that Ca^{2+} increases the maximal level of IP_3R channel activity without changing the affinity of IP_3R for IP_3.

In the former mechanism, the maximal Ca^{2+} release rate at saturating IP_3 concentrations should be independent of the Ca^{2+} concentration, although the EC_{50} for IP_3 should decrease with increasing Ca^{2+} concentration. However, in the latter case, the maximum level of IP_3R activation cannot be attained at low Ca^{2+} concentrations even with saturating concentrations of IP_3, and the EC_{50} for IP_3 should be constant regardless of the Ca^{2+} concentration.

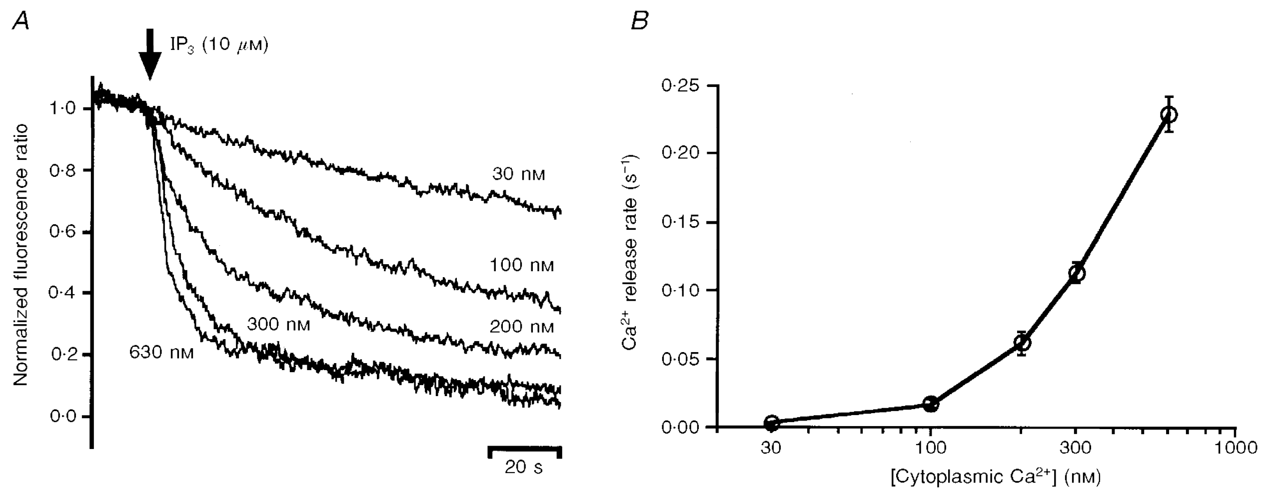

Figure 1. IP_3-induced Ca^{2+} release at various cytoplasmic Ca^{2+} concentrations

A, time courses of Ca^{2+} release at the indicated cytoplasmic Ca^{2+} concentrations. Application of 10 μM IP_3 was started at the time point indicated by the arrow. *B*, the initial rate of Ca^{2+} release was plotted against the cytoplasmic Ca^{2+} concentration (mean ± S.E.M., $n = 5$).

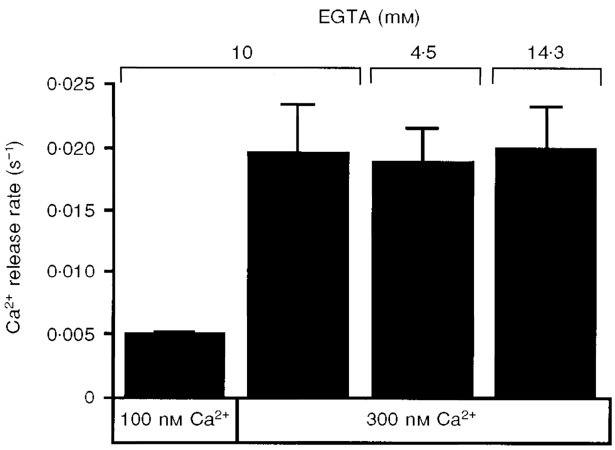

Figure 2. Extent of Ca^{2+}-mediated potentiation of IP_3-induced Ca^{2+} release is independent of EGTA concentration

The total EGTA concentration at 300 nM Ca^{2+} was changed from 10 mM to either 4·5 mM or 14·3 mM for adjustment of the concentration of Ca^{2+}-bound or Ca^{2+}-unbound EGTA, respectively, to that at 100 nM Ca^{2+}. The IP_3 concentration was 100 nM. Means ± S.E.M., $n = 5$.

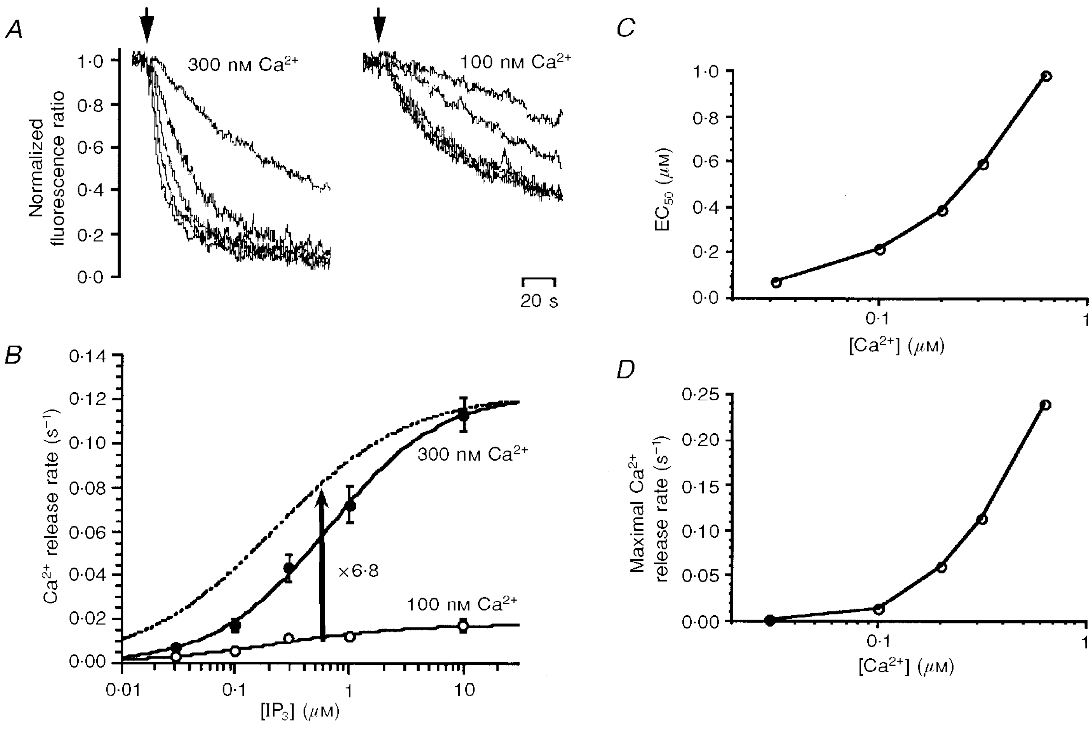

Figure 3. Ca^{2+} concentration dependence of IP_3-induced Ca^{2+} release

A, time course of Ca^{2+} release induced by IP_3 at cytoplasmic Ca^{2+} concentrations of 300 nM (left) and 100 nM (right). *B*, the Ca^{2+} release rate was calculated from experimental results similar to those in *A* and plotted against the IP_3 concentration. Open and filled circles represent Ca^{2+} release rates at 100 and 300 nM Ca^{2+}, respectively. The data were fitted by Hill's equation to give continuous curves. The fitted curve for 100 nM Ca^{2+} was scaled up 6·8-fold (dotted curve). *C*, the IP_3 concentration required for half-maximal activation of Ca^{2+} release (EC_{50}) was plotted against the cytoplasmic Ca^{2+} concentration. *D*, the maximal Ca^{2+} release rate was plotted against the Ca^{2+} concentration.

To test the above hypotheses, we compared the IP_3 dependence of Ca^{2+} release at high and low concentrations of Ca^{2+}. Ca^{2+} was released at various concentrations of IP_3 at both 300 and 100 nM Ca^{2+} (Fig. 3*A*). At 300 nM Ca^{2+}, the rate of Ca^{2+} release increased markedly with increasing concentration of IP_3, whereas at 100 nM Ca^{2+}, the effect of an increase in the concentration of IP_3 was far weaker. Figure 3*B* shows the relationship between IP_3 concentration and initial rate of Ca^{2+} release at 100 and 300 nM Ca^{2+}. We fitted Hill's equation to the data points,

$$r_{max}[Ca^{2+}]^n/([Ca^{2+}]^n + K^n),$$

where r_{max}, K and n represent maximal Ca^{2+} release rate, Ca^{2+} concentration required for half-maximal activation of Ca^{2+} release (EC_{50}), and Hill coefficient, respectively. r_{max} was ~6·8 times higher at 300 nM Ca^{2+} than at 100 nM Ca^{2+}. Vertical scaling of the IP_3 dependence curve at 100 nM Ca^{2+} (dotted line in Fig. 3*B*) by 6·8 times shows that the EC_{50} for IP_3 was higher at 300 nM Ca^{2+} than at 100 nM Ca^{2+}.

We conducted similar experiments at various cytoplasmic Ca^{2+} concentrations and derived the relationship between the EC_{50} for IP_3 and the Ca^{2+} concentration shown in Fig. 3*C*. The EC_{50} for IP_3 increased from 0·07 to 1·0 μM with increasing cytoplasmic Ca^{2+} concentration from 30 to 630 nM. The maximal Ca^{2+} release rate also increased 110-fold with increasing concentration of Ca^{2+} (Fig. 3*D*), indicating that the activity of Ca^{2+} release channels is enhanced by Ca^{2+} even at a saturating concentration of IP_3. In the presence of a low cytoplasmic Ca^{2+} concentration (below 100 nM), IP_3 very weakly induced Ca^{2+} release. These results are inconsistent with the two extreme cases that we initially considered.

Both Ca^{2+} and IP_3 are required for maximal IP_3R activation

To obtain a further understanding of how IP_3R is activated, we replotted the Ca^{2+} release rate against the Ca^{2+} and IP_3 concentrations in a three-dimensional graph (Fig. 4*A*, spheres). It is obvious that the Ca^{2+} release rate increased markedly only when both the Ca^{2+} and the IP_3 concentration were increased. Neither Ca^{2+} nor IP_3 induced Ca^{2+} release in the absence of the other. These results indicate that Ca^{2+} and IP_3 are simultaneously required for IP_3R activation in smooth muscle cells.

DISCUSSION

In this study, we found that the submicromolar Ca^{2+}-mediated potentiation of Ca^{2+} release via IP_3R is not caused by an increase in the affinity of IP_3R for IP_3, and that cytoplasmic Ca^{2+} and IP_3 are simultaneously required for the gating of the IP_3R Ca^{2+} release channel. We showed that the cytoplasmic Ca^{2+} concentration in a submicromolar range determines the level of IP_3R activity at near-saturating IP_3 concentrations and that at the same time the increasing Ca^{2+} concentration lowers the affinity of IP_3R for IP_3 (Fig. 3).

Four-state model of IP_3R activation

We constructed a minimum steady-state model to account for the observed features of IP_3-induced Ca^{2+} release. The essential property of the model is that the binding of either Ca^{2+} or IP_3 alone to the IP_3R does not induce IP_3R activation, but simultaneous binding of both Ca^{2+} and IP_3 to IP_3R leads to IP_3R activation. We speculated that this simultaneous binding is essential, based on our finding that the rate of Ca^{2+} release is extremely low, even at an IP_3 concentration as high as 10 μM, when the Ca^{2+} concentration is low (Figs 3*D* and 4*A*). Another important feature of our model is that the binding of Ca^{2+} and IP_3 to IP_3R is allosterically controlled by the binding of IP_3 and Ca^{2+}, respectively. We included this in our model, based on our finding that the EC_{50} for IP_3 increased with increasing Ca^{2+} concentration (Fig. 3*C*). We noted a similar change in the Ca^{2+} dependence of Ca^{2+} release with an increase in the IP_3 concentration (data not shown). A four-state model that accommodates the above considerations is shown in Fig. 4*B*. The stoichiometry of IP_3 and Ca^{2+} binding was assumed to be *m* and *n*, respectively. The channel is open only in the Ca^{2+}- and IP_3-bound state. The Ca^{2+} release rate is thus described as:

$$r_{max}[Ca^{2+}]^n[IP_3]^m/([Ca^{2+}]^n[IP_3]^m + [Ca^{2+}]^n K_2{}^m + [IP_3]^m K_3{}^n + K_1{}^n K_2{}^m),$$

where r_{max} is the maximal Ca^{2+} release rate, K_1 and K_3 are the K_d for Ca^{2+} binding to IP_3-unbound and -bound IP_3R, respectively, and K_2 is the K_d for IP_3 binding to Ca^{2+}-unbound IP_3R. We found that the model describes the important features of the experimental data (Fig. 4*A*, curved surface). Using a least-squares fitting method of a mathematics software package (Mathematica, Worfram Research, Inc., IL, USA) running on a personal computer, we obtained the following parameter values for each reaction: K_1, ~154 nM; K_2, ~1·6 μM; K_3, ~403 nM; K_4 (the K_d for IP_3 binding to Ca^{2+}-bound IP_3R), ~201 nM; *m*, ~1; and *n*, ~2. According to this model, a Ca^{2+}-bound IP_3R has about 8-fold lower affinity for IP_3 than does a Ca^{2+}-unbound IP_3R. The affinity of the IP_3R for Ca^{2+} also decreased about 2·5-fold upon binding of IP_3.

Although our model successfully describes the present experimental data, it does not describe all the features of the Ca^{2+} dependence of IP_3R within the entire physiological range of Ca^{2+} concentrations. At micromolar concentrations, Ca^{2+} has an inhibitory effect on IP_3R activity (Iino, 1990; Bezprozvanny *et al.* 1991; Finch *et al.* 1991; Bootman *et al.* 1995). Unfortunately we could not study the Ca^{2+}-mediated inhibition due to current experimental limitations. There are several possible ways in which the present model could be modified to include the inhibitory effect of Ca^{2+}. One model is that Ca^{2+} binding to an inhibitory site alters the equilibrium of the four states in our model, so lowering the affinity of Ca^{2+} and/or IP_3 for their respective activation sites, resulting in a decreased population of active IP_3Rs

(allosteric inhibition). In another model, the binding of Ca^{2+} to the inhibitory site occurs only in the IP_3R that binds Ca^{2+} at activation sites and IP_3 (sequential inhibition). Clearly we need more information to discriminate between these and other possibilities.

Comparison of the present results with those of the IP_3 binding studies

Several biochemical reports regarding Ca^{2+}-mediated regulation of IP_3 binding to the IP_3R have been published. Benevolensky *et al.* demonstrated the presence of high- and low-affinity IP_3 binding sites in sarcoplasmic reticulum

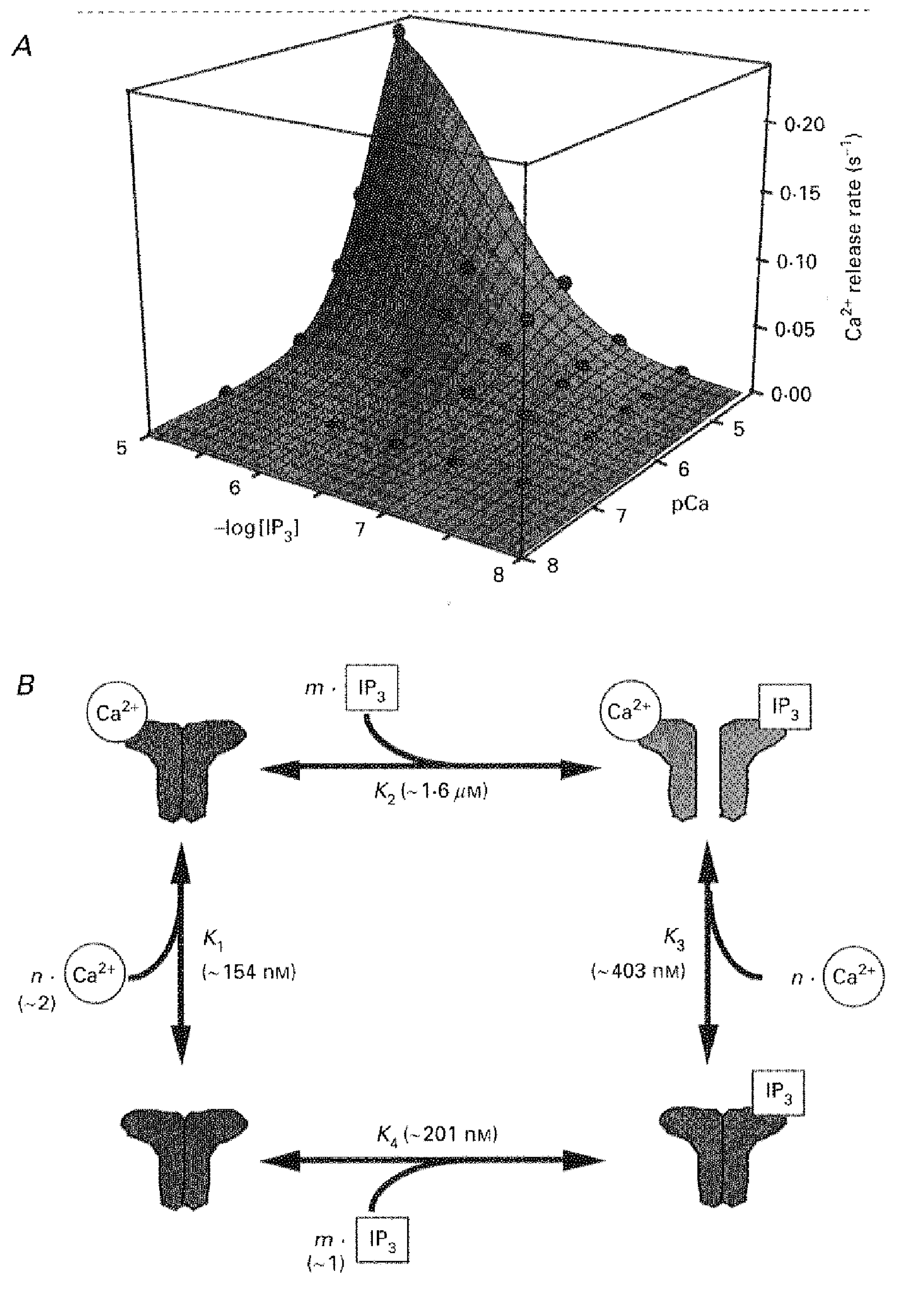

Figure 4. Allosteric activation of IP_3 receptors by Ca^{2+} and IP_3

A, the Ca^{2+} release rate was plotted against the Ca^{2+} and IP_3 concentrations. Experimental data (spheres) are fitted by the equation described in *B*, as shown by the curved surface. *B*, a possible mechanism of IP_3 receptor activation. The channel has n Ca^{2+} binding sites and m IP_3 binding sites. K_1 and K_3 represent K_d for Ca^{2+} binding to IP_3-unbound and IP_3-bound forms of the receptor, respectively. K_2 and K_4 represent K_d for IP_3 binding to Ca^{2+}-unbound and Ca^{2+}-bound forms of the receptor, respectively.

vesicles from aortic smooth muscle (Benevolensky, Moraru & Watras, 1994). The K_d of the low-affinity binding sites, accounting for > 90% of the total IP_3 binding sites, depended on the cytoplasmic Ca^{2+} concentration. The K_d was 49·3 nM in the absence of Ca^{2+} and 155 nM in the presence of 2 μM Ca^{2+}. Similar Ca^{2+}-mediated inhibition of IP_3 binding has been detected in cerebellar IP_3R (Worley, Baraban, Supattapone, Wilson & Snyder, 1987; Hannaert-Merah, Coquil, Combettes, Claret, Mauger & Champeil, 1994). Only a single class of IP_3 binding sites was detected in IP_3R purified from human IP_3R type 1 synthesized in a baculovirus expression vector system, and a Ca^{2+}-dependent increase in K_d for IP_3, from 79 nM at 3 nM Ca^{2+} to 312 nM at 1·4 μM Ca^{2+}, has been reported (Yoneshima, Miyawaki, Michikawa, Furuichi & Mikoshiba, 1997). There are, however, contradictory results for several cell types, in which an increase in the Ca^{2+} concentration causes a decrease in K_d for IP_3 (Marshall & Taylor, 1994). The effect of Ca^{2+} is complicated in rat basophilic leukaemia (RBL) cells, which have low- and high-affinity IP_3 binding sites. An increase in the Ca^{2+} concentration from 100 to 500 nM results both in the conversion of a portion of the low-affinity sites to high-affinity sites and an increase in the K_d of the low-affinity sites (Watras, Moraru, Costa & Kindman, 1994). The K_d for IP_3 binding to IP_3R type 3 decreased with an increase in Ca^{2+} concentration (Yoneshima *et al.* 1997). Thus, the mode of Ca^{2+}-dependent IP_3 binding may depend on the subtype of the IP_3R and/or cell type-specific post-translational modification of the IP_3R. IP_3R type 1 seems to be dominantly expressed in smooth muscle cells (Chadwick, Saito & Fleischer, 1990; De Smedt *et al.* 1994; Islam, Yoshida, Koga, Kojima, Kangawa & Imai, 1996). If this is also the case in guinea-pig portal vein, the present results seem to be in general agreement with the results of binding studies, in that the lowering of the sensitivity for IP_3 is accompanied by an increase in the Ca^{2+} concentration. It would be interesting to examine the Ca^{2+} dependence of IP_3-induced Ca^{2+} release in cells expressing only IP_3R type 3.

Physiological significance of the requirement for both Ca^{2+} and IP_3 for IP_3R activation

The properties of the IP_3R revealed in the present study are consistent in many ways with the role of IP_3R as one of the key components for inducing Ca^{2+} oscillations. Firstly, in the presence of low concentrations of Ca^{2+}, high concentrations of IP_3 activate IP_3R only weakly. This is consistent with the baseline Ca^{2+} oscillations which are a characteristic pattern of Ca^{2+} oscillations seen in many cell types (Berridge, 1993). In these baseline Ca^{2+} oscillations, after each Ca^{2+} spike the Ca^{2+} concentration returns to the baseline level. During the period between two successive spikes, the Ca^{2+} release rate should remain low in the presence of IP_3. This may be enabled by the low level of IP_3R activity in the presence of a low concentration of Ca^{2+}. Secondly, the Ca^{2+} concentration dependence of the Ca^{2+} release rate had a Hill coefficient of ~2 (also, $n \approx 2$ in our model fitting), suggesting that IP_3R activation requires simultaneous binding of two Ca^{2+} ions. The strong Ca^{2+} concentration dependence is advantageous for generation of Ca^{2+} spikes. Thirdly, the extent of Ca^{2+}-mediated control of IP_3R activity is IP_3 concentration-dependent. In the presence of a low concentration of IP_3, Ca^{2+} alone activates the IP_3R so weakly that Ca^{2+} spikes are not generated. With an increase in the IP_3 concentration, Ca^{2+} becomes effective in inducing Ca^{2+} release. This IP_3 requirement may explain the requirement for receptor activation to start the cytoplasmic Ca^{2+} oscillation.

It seems pertinent here to mention mechanisms other than Ca^{2+}-mediated potentiation of IP_3R activity that participate in the generation of Ca^{2+} oscillations. Firstly, the falling phase of the Ca^{2+} oscillation clearly requires inhibitory mechanisms of Ca^{2+} release that are still elusive. One possible mechanism for the termination of each Ca^{2+} oscillation may be the depletion of the Ca^{2+} stores, which results in a decreased Ca^{2+} flux rate and a decrease in the extent of Ca^{2+}-mediated positive feedback. Another candidate mechanism may be Ca^{2+}-mediated inhibition of IP_3R (Iino, 1990; Bezprozvanny *et al.* 1991; Finch *et al.* 1991; Bootman *et al.* 1995). After Ca^{2+} spikes are generated, the Ca^{2+} concentration around the Ca^{2+} stores may become high enough to terminate Ca^{2+} release via the Ca^{2+}-mediated inhibitory mechanism. Secondly, CICR mechanism via RyRs may be involved in the Ca^{2+} oscillations and waves, as is the case in striated muscle cells (Endo *et al.* 1970; Takamatsu & Wier, 1990). Because activation of CICR has been shown to require a higher Ca^{2+} concentration than activation of IP_3R (Iino, 1989), CICR has the potential to play a role in the amplification of Ca^{2+} release after the IP_3R is activated. However, RyRs are not always expressed in cells in which the production of IP_3 is required for the generation of Ca^{2+} oscillations and waves. Furthermore, CICR in smooth muscle cells that express RyRs contributes little in the generation of Ca^{2+} waves (Iino, Yamazawa, Miyashita, Endo & Kasai, 1993).

In conclusion, the requirement for both Ca^{2+} and IP_3 for IP_3R activation is important for the generation of Ca^{2+} spikes and Ca^{2+} oscillations, in which a multitude of molecular mechanisms are involved.

Benevolensky, D., Moraru, I. I. & Watras, J. (1994). Micromolar calcium decreases affinity of inositol trisphosphate receptor in vascular smooth muscle. *Biochemical Journal* **299**, 631–636.

Berridge, M. J. (1993). Inositol trisphosphate and calcium signalling. *Nature* **361**, 315–325.

Bezprozvanny, I., Watras, J. & Ehrlich, B. E. (1991). Bell-shaped calcium-response curve of Ins(1,4,5)P_3- and calcium-gated channels from endoplasmic reticulum of cerebellum. *Nature* **351**, 751–754.

Bootman, M. D., Missiaen, L., Parys, J. B., De Smedt, H. & Casteels, R. (1995). Control of inositol 1,4,5-trisphosphate-induced Ca^{2+} release by cytosolic Ca^{2+}. *Biochemical Journal* **306**, 445–451.

Chadwick, C. C., Saito, A. & Fleischer, S. (1990). Isolation and characterization of the inositol trisphosphate receptor from smooth muscle. *Proceedings of the National Academy of Sciences of the USA* **87**, 2132–2136.

De Smedt, H., Missiaen, L., Parys, J. B., Bootman, M. D., Mertens, L., Van Den Bosch, L. & Casteels, R. (1994). Determination of relative amounts of inositol trisphosphate receptor mRNA by ratio polymerase chain reaction. *Journal of Biological Chemistry* **269**, 21691–21698.

Endo, M., Tanaka, M. & Ogawa, Y. (1970). Calcium induced release of calcium from the sarcoplasmic reticulum of skinned skeletal muscle fibres. *Nature* **228**, 34–36.

Finch, E. A., Turner, T. J. & Goldin, S. M. (1991). Calcium as a coagonist of inositol 1,4,5-trisphosphate-induced calcium release. *Science* **252**, 443–446.

Golovina, V. A. & Blaustein, M. P. (1997). Spatially and functionally distinct Ca^{2+} stores in sarcoplasmic and endoplasmic reticulum. *Science* **275**, 1643–1648.

Hannaert-Merah, Z., Coquil, J. F., Combettes, L., Claret, M., Mauger, J. P. & Champeil, P. (1994). Rapid kinetics of myo-inositol trisphosphate binding and dissociation in cerebellar microsomes. *Journal of Biological Chemistry* **269**, 29642–29649.

Hirose, K. & Iino, M. (1994). Heterogeneity of channel density in inositol-1,4,5-trisphosphate-sensitive Ca^{2+} stores. *Nature* **372**, 791–794.

Hoffer, A. M., Schlue, W. R., Curci, S. & Machen, T. E. (1995). Spatial distribution and quantitation of free luminal [Ca] within the $InsP_3$-sensitive internal store of individual BHK-21 cells: ion dependence of $InsP_3$-induced Ca release and reloading. *FASEB Journal* **9**, 788–798.

Iino, M. (1989). Calcium-induced calcium release mechanism in guinea pig taenia caeci. *Journal of General Physiology* **94**, 363–383.

Iino, M. (1990). Biphasic Ca^{2+} dependence of inositol 1,4,5-trisphosphate-induced Ca release in smooth muscle cells of the guinea pig taenia caeci. *Journal of General Physiology* **95**, 1103–1122.

Iino, M. & Endo, M. (1992). Calcium-dependent immediate feedback control of inositol 1,4,5-triphosphate-induced Ca^{2+} release. *Nature* **360**, 76–78.

Iino, M., Yamazawa, T., Miyashita, Y., Endo, M. & Kasai, H. (1993). Critical intracellular Ca^{2+} concentration for all-or-none Ca^{2+} spiking in single smooth muscle cells. *EMBO Journal* **12**, 5287–5291.

Islam, M. O., Yoshida, Y., Koga, T., Kojima, M., Kangawa, K. & Imai, S. (1996). Isolation and characterization of vascular smooth muscle inositol 1,4,5-trisphosphate receptor. *Biochemical Journal* **316**, 295–302.

Marshall, I. C. & Taylor, C. W. (1994). Two calcium-binding sites mediate the interconversion of liver inositol 1,4,5-trisphosphate receptors between three conformational states. *Biochemical Journal* **301**, 591–598.

Richardson, A. & Taylor, C. W. (1993). Effects of Ca^{2+} chelators on purified inositol 1,4,5-trisphosphate ($InsP_3$) receptors and $InsP_3$-stimulated Ca^{2+} mobilization. *Journal of Biological Chemistry* **268**, 11528–11533.

Takamatsu, T. & Wier, W. G. (1990). Calcium waves in mammalian heart: quantification of origin, magnitude, waveform, and velocity. *FASEB Journal* **4**, 1519–1525.

Watras, J., Moraru, I., Costa, D. J. & Kindman, L. A. (1994). Two inositol 1,4,5-trisphosphate binding sites in rat basophilic leukemia cells: relationship between receptor occupancy and calcium release. *Biochemistry* **33**, 14359–14367.

Worley, P. F., Baraban, J. M., Supattapone, S., Wilson, V. S. & Snyder, S. H. (1987). Characterization of inositol trisphosphate receptor binding in brain. Regulation by pH and calcium. *Journal of Biological Chemistry* **262**, 12132–12136.

Yoneshima, H., Miyawaki, A., Michikawa, T., Furuichi, T. & Mikoshiba, K. (1997). Ca^{2+} differentially regulates the ligand-affinity states of type 1 and type 3 inositol 1,4,5-trisphosphate receptors. *Biochemical Journal* **322**, 591–596.

Acknowledgements

The authors thank Y. Hirose for technical assistance. This work was supported by grants from the Ministry of Education, Science and Culture of Japan and the Uehara Memorial Foundation.

Corresponding author

K. Hirose: Department of Pharmacology, Faculty of Medicine, The University of Tokyo, 7-3-1 Hongo, Bunkyo-ku, Tokyo 113, Japan.

Email: hirose@calcium.cmp.m.u-tokyo.ac.jp